Electronic properties of icosahedral quasicrystals in Mg-Al-Ag, Mg-Al-Cu and Mg-Zn-Ga alloy systems

1990 J. Phys.: Condens. Matter 2 6153

(http://iopscience.iop.org/0953-8984/2/28/006)

J. Phys.: Condens. Matter **2** (1990) 6153–6167. Printed in the UK

Electronic properties of icosahedral quasicrystals in Mg–Al–Ag, Mg–Al–Cu and Mg–Zn–Ga alloy systems

U Mizutani†, Y Sakabe† and T Matsuda‡

† Department of Crystalline Materials Science, Nagoya University, Furo-cho, Chikusa-ku, Nagoya 464-01, Japan

‡ Department of Physics, Aichi University of Education, Kariya-shi, Aichi 448 Japan

Received 13 October 1989, in final form 19 February 1990

Abstract. The electronic structure and the electron transport properties of sp-electron quasicrystals have been studied, using in total, 20 quasicrystals in the three alloy systems Mg–Al–Ag, Mg–Al–Cu and Mg–Zn–Ga. We revealed that the temperature dependence of the electrical resistivity changes its characteristic features with increasing resistivity in the same manner as that in the non-magnetic amorphous alloys. This is apparently consistent with the generalised Faber–Ziman theory, but this simple model poses difficulties in explaining a definite increase in the resistivity upon improvement in the quasicrystallinity, brought about by the heat-treatment of the $Mg_{39.5}Zn_{40}Ga_{20.5}$ quasicrystal. The Hall coefficient exhibits the sizable temperature dependence when its magnitude deviates from the free electron value, suggesting the important role of the Fermi surface–Brillouin zone interaction. The temperature dependence of the thermoelectric power below 300 K is found to be non-linear, as opposed to a more linear one in the amorphous alloy. The electronic specific heat coefficient plotted against the electron concentration e/a exhibits a universal trend regardless of the alloy system and decreases with decreasing e/a from the free electron value to about one-third of the free electron value. It is noted that a thermally stable quasicrystal apparently possesses a reduced electronic specific heat coefficient.

1. Introduction

The atomic structure of icosahedral quasicrystals has been extensively studied and has now been well documented (see, for example, Steinhardt and Ostlund 1987). The atomic structure is divided into two groups in terms of the structural unit involved in building up the quasiperiodic three-dimensional Penrose tiling: one described by the Mackay icosahedron containing 54 atoms and the other by the triacontahedron containing 45 atoms. The former is apparently best suited to describe the atomic structure in the family of the Al–Mn type quasicrystals, whereas the latter possesses the same local symmetry as that of the Frank–Kasper phase and is suited to describe the atomic structure of the Mg based quasicrystals.

The Mg based quasicrystals are of particular interest from the viewpoint of electron transport, since the Fermi level is located in the sp band and is free from any magnetic effect and from the d-electron conduction. These electronically simple quasicrystals are considered to be of prime importance in studying the scattering mechanism of conduction electrons travelling in the quasiperiodic lattice (Wagner *et al* 1988, Bruhwiler 1988, Matsuda *et al* 1989, 1990). Extensive experimental studies under the same guiding

0953-8984/90/286153 + 15 $03.50

principle have been made for the sp-electron amorphous alloys and the scattering mechanism involved has been elucidated (Mizutani 1988a, b).

In the present study, we prepared a large number of Mg based quasicrystalline alloys by the melt-spinning technique and studied the electronic structure and the electron transport properties. The results are discussed in comparison with the data for the sp-electron amorphous alloys.

2. Experimental procedure

The quasicrystalline alloys were prepared in the three Mg based ternary alloy systems: Mg–Al–Ag, Mg–Al–Cu and Mg–Zn–Ga. All these alloy ingots were obtained by induction-melting appropriate amounts of constituent elements 99.95%Mg, 99.999%Al, 99.999%Zn, 99.999%Cu, 99.999%Ga and 99.999%Ag in a high-purity graphite crucible under a pressurised He atmosphere. Ribbon specimens were fabricated by melt-spinning onto a copper wheel at a tangential speed of less than 62 ms^{-1}. A quasicrystalline single phase has been confirmed by both electron diffraction and x-ray diffraction with Cu Kα radiation.

The low-temperature specific heat, the electrical resistivity, the Hall coefficient and the thermoelectric power have been measured in the temperature range 1.5–6 K, 2–600 K, 77–300 K and 78–570 K, respectively. The DC adiabatic method was employed for the specific heat measurements. Both resistivity and the Hall coefficient were measured, using four- and five-terminal DC methods, respectively. A major error in determining the value of ρ and R_H at room temperature originated from the lack of uniformity in ribbon thickness. The average value was determined by measuring the value for more than five identical specimens. The integral method was employed for the thermoelectric power measurements. The density was measured by the Archimedes method using xylene as a fluid.

3. Results

Low-temperature specific heat data are summarised in table 1. Numerical data for the electron transport properties and the mass density in the three Mg based alloy systems are listed in table 2. The details of these results are described below for the respective alloy systems.

3.1. Mg–Al–Ag

The formation of a quasicrystalline single phase in the Mg–Al–Ag alloy system by melt-spinning method was first reported by Inoue *et al* (1988). Figure 1 shows the composition diagram showing the formation of both quasicrystalline and amorphous phases obtained by the present experiment, along with the data reported by Inoue *et al*. We obtained both amorphous and quasicrystalline single phases in the two series of the alloy formula $Mg_{90-x}Al_xAg_{10}$ and $Mg_{80-x}Al_xAg_{20}$ with $20 \leqslant x \leqslant 45$ and $20 \leqslant x \leqslant 50$, respectively. Here, the alloys $Mg_{70}Al_{20}Ag_{10}$ and $Mg_{60}Al_{20}Ag_{20}$ turned out to be in an amorphous single phase, whereas the rest were in a quasicrystalline single phase.

The low-temperature specific heat data in the temperature range 1.5–5 K can be well fitted to a conventional equation

$$C = \gamma T + \alpha T^3 + \delta T^5 \tag{1}$$

where γ is the electronic specific heat coefficient and α and δ are the lattice specific heat

Table 1. Low temperature specific heat data for Mg–Al–Ag, Mg–Al–Cu and Mg–Zn–Ga quasicrystalline alloys.

	γ (mJ mol^{-1} K^{-2})	α (10^{-2} mJ mol^{-1} K^{-4})	θ_D (K)	δ (10^{-4} mJ mol^{-1} K^{-6})	γ^{free} (mJ mol^{-1} K^{-2})	γ/γ^{free}
$Mg_{70}Al_{20}Ag_{10}$†	1.17 ± 0.01	5.0 ± 0.2	340 ± 3	7.3 ± 0.5	0.94	1.24
$Mg_{50}Al_{40}Ag_{10}$	1.15 ± 0.01	4.1 ± 0.2	361 ± 4	3.4 ± 0.5	0.92	1.25
$Mg_{30}Al_{50}Ag_{20}$	1.08 ± 0.02	5.4 ± 0.2	331 ± 5	5.9 ± 0.8	0.90	1.20
$Mg_{35.8}Al_{51.9}Cu_{12.3}$	1.15 ± 0.01	3.2 ± 0.1	393 ± 4	−0.6 ± 0.4	0.90	1.28
$Mg_{39.5}Al_{48.2}Cu_{12.3}$	1.19 ± 0.01	2.6 ± 0.1	420 ± 7	2.8 ± 0.5	0.90	1.32
$Mg_{43.2}Al_{44.5}Cu_{12.3}$	1.17 ± 0.01	1.6 ± 0.1	500 ± 10	5.4 ± 0.4	0.90	1.30
$Mg_{39.5}Al_{54.0}Cu_{6.5}$	1.38 ± 0.01	2.1 ± 0.2	460 ± 10	7.1 ± 0.5	0.92	1.50
$Mg_{39.5}Al_{51.1}Cu_{9.4}$	1.17 ± 0.01	3.0 ± 0.2	402 ± 7	1.0 ± 0.5	0.92	1.27
$Mg_{39.5}Al_{45.3}Cu_{15.2}$	1.11 ± 0.01	1.5 ± 0.2	500 ± 20	5.4 ± 0.5	0.88	1.26
$Mg_{39.5}Zn_{40.0}Ga_{20.5}$	0.99 ± 0.01	3.1 ± 0.2	398 ± 8	16 ± 1	0.87	1.14
$Mg_{33.5}Zn_{40.0}Ga_{26.5}$	0.91 ± 0.01	4.4 ± 0.2	353 ± 5	17 ± 1	0.87	1.05
$Mg_{33.5}Zn_{46.0}Ga_{20.5}$	0.80 ± 0.01	4.0 ± 0.2	365 ± 6	18 ± 1	0.86	0.93
$Mg_{36.5}Zn_{43.0}Ga_{20.5}$	0.82 ± 0.01	4.6 ± 0.1	348 ± 4	11 ± 1	0.86	0.96

† This sample is in the amorphous single phase.

Table 2. Electron transport properties and mass density for Mg–Al–Ag, Mg–Al–Cu and Mg–Zn–Ga quasicrystalline alloys

	x	ρ(300K) ($\mu\Omega$cm)	R_H (10^{-11} m^3 A^{-1} s^{-1})	R_H^{free} (10^{-11} m^3 A^{-1} s^{-1})	TCH (10^{-4}K^{-1})	S(300K) (μV K^{-1})	A (g mol^{-1})	d (g cm^{-3})
$Mg_{90-x}Al_xAg_{10}$								
	20†	78 ± 4	−5.8 ± 0.5	−6.2	1.18	−1.62	33.23	2.66
	30	81 ± 3	−5.6 ± 0.5	−5.7	—	2.53	33.46	2.76
	35	88 ± 2	−6.1 ± 0.3	−5.6	—	−5.18	33.60	2.78
	40	90 ± 4	−6.7 ± 0.6	−5.2	7.34	−5.45	33.73	2.90
	45	91 ± 3	−6.4 ± 0.7	−5.1	—	−5.10	33.87	2.93
$Mg_{80-x}Al_xAg_{20}$								
	20†	128 ± 3	−5.7 ± 0.4	−6.4	—	−0.09	41.55	3.39
	30	157 ± 6	—	−6.0	—	—	41.82	3.47
	40	139 ± 4	−5.8 ± 0.4	−5.4	—	—	42.09	3.67
	50	111 ± 7	−6.1 ± 0.4	−5.1	6.50	−1.95	42.36	3.76
$Mg_xAl_{87.7-x}Cu_{12.3}$								
	35.8	70 ± 7	−4.7 ± 0.3	−4.8	0.01	−5.2	30.77	2.79
	39.5	81 ± 1	−5.9 ± 0.4	−4.8	1.66	−5.3	30.42	2.76
	43.2	86 ± 3	−7.3 ± 0.7	−4.9	10.57	−5.4	30.32	2.73
$Mg_{39.5}Al_{60.5-x}Cu_x$								
	6.5	65 ± 2	−4.4 ± 0.4	−4.7	—	−5.1	28.30	2.52
	9.4	72 ± 4	−4.8 ± 0.1	−4.8	−1.06	−5.4	29.36	2.61
	15.2	88 ± 2	−6.7 ± 0.1	−4.9	5.68	−6.0	31.48	2.89
$Mg_{60-x}Zn_{40}Ga_x$								
	17.5	140 ± 7	−5.2 ± 0.7	−5.2	0.65	−2.1	48.69	4.54
	20.5	143 ± 3	−8.1 ± 1.0	−5.1	—	−6.1	50.05	4.61
	23.5	150 ± 11	−10.1 ± 0.9	−5.1	−0.28	−7.3	51.41	4.71
	26.5	154 ± 5	−14.9 ± 0.9	−4.9	31.11	−8.2	52.77	4.91
$Mg_{39.5}Zn_{60.5-x}Ga_x$								
	18.0	149 ± 9	−7.2 ± 0.5	−4.9	—	−4.7	49.94	4.66
	23.0	139 ± 5	−8.8 ± 0.5	−5.1	—	−5.1	50.16	4.56
$Mg_{79.5-x}Zn_xGa_{20.5}$								
	43.0	157 ± 2	−9.7 ± 0.6	−5.0	—	—	51.20	4.82
	46.0	183 ± 3	−10.7 ± 0.3	−5.1	—	−6.3	52.51	4.87

† These samples are in the amorphous single phase.

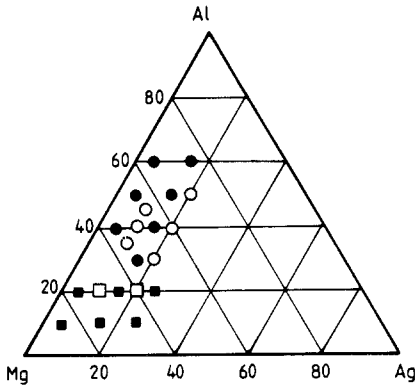

Figure 1. Composition range for the formation of the icosahedral quasicrystalline single phase (○): present results; (●): Inoue *et al* (1988) and the amorphous single phase; (□): present results; (■): Inoue *et al* (1988) in the Mg–Al–Ag alloy system.

coefficients. The value of γ can be calculated on the basis of the free electron model by inserting the measured density d, the average atomic weight A and the average electron concentration e/a into the expression

$$\gamma_{\text{free}} = 0.136(A/d)^{2/3}(e/a)^{1/3} \tag{2}$$

where e/a is calculated by assuming that Ag, Mg and Al contribute 1, 2 and 3 free electrons per atom, respectively. The ratio $\gamma_{\text{exp}}/\gamma_{\text{free}}$ turns out to be around 1.2. This indicates that the free electron model holds well in the quasicrystalline phase, since the factor 0.2 can be reasonably attributed to the electron–phonon enhancement effect. The Debye temperature θ_D is calculated from α through the relation:

$$\theta_D = (12\pi^4 R/5\alpha)^{1/3} \tag{3}$$

where R is the gas constant.

The temperature dependence of the electrical resistivity for the representative Mg–Al–Ag alloys is shown in figure 2 over the temperature range 2–300 K. Its inset shows the resistivity at 300 K as a function of Al content for these alloys in both amorphous and quasicrystalline phases. The values for $Mg_{80-x}Al_xAg_{20}$ are consistently higher than those for $Mg_{90-x}Al_xAg_{10}$ alloys. Inoue *et al* (1988) reported the resistivity values for $Mg_{75-x}Al_xAg_{15}$, which are incorporated in the inset. There exists no striking difference in the ρ–T characteristics between the amorphous and quasicrystalline phases.

The Hall coefficient R_H at 300 K and its temperature dependence in the range 77–300 K are shown in figure 3. Included is the corresponding free electron value. The Hall coefficient reduces its absolute magnitude with increasing temperature for the $Mg_{50}Al_{40}Ag_{10}$ quasicrystal, whereas the temperature dependence is apparently absent in the $Mg_{70}Al_{20}Ag_{10}$ amorphous alloy. As will be shown later, the temperature dependence of the Hall coefficient in sp-electron quasicrystals is generally more prominent than that in the sp-electron amorphous alloys but not necessarily a feature observed in common to all quasicrystals.

The thermoelectric power for both quasicrystalline and amorphous alloys is plotted in figure 4 as a function of temperature over the range 78–570 K. The temperature dependence of the thermoelectric power in the amorphous alloy is small and linear below 300 K. However, the non-linear temperature dependence even below 300 K is clearly seen for all quasicrystalline alloys. The data below 300 K may well be approximated by two straight lines which intersect at a temperature T_b, as denoted by an arrow in figure 4.

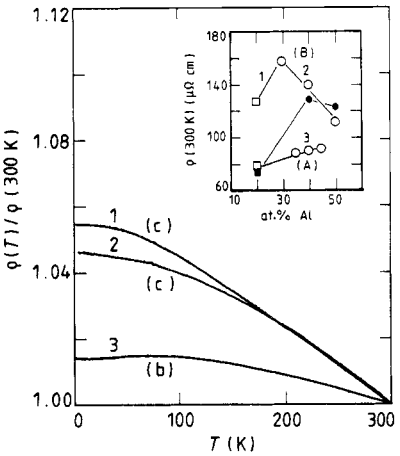

Figure 2. Temperature dependence of the electrical resistivity normalised with respect to that at 300 K for the quasicrystalline and amorphous Mg–Al–Ag alloys. The number denotes the identification of the sample shown in the inset. The letters (A) and (B) refer to the alloy series $Mg_{90-x}Al_xAg_{10}$ and $Mg_{80-x}Al_xAg_{20}$, respectively. Open squares and circles represent the data for the amorphous and quasicrystalline samples, respectively. Full circles represent the data for the $Mg_{85-x}Al_xAg_{15}$ obtained by Inoue *et al* (1988). Letters (b) and (c) marked for the ρ–T curves denote the ρ–T types discussed in section 4.1.

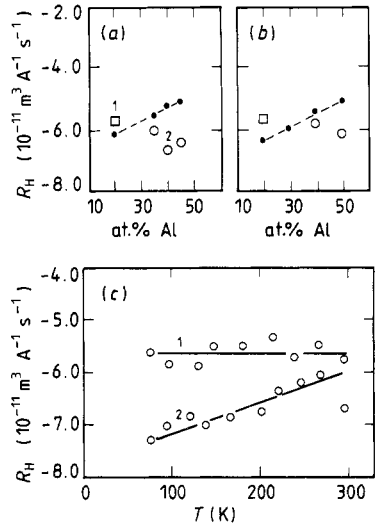

Figure 3. Al concentration dependence of the Hall coefficient at 300 K for (*a*) $Mg_{90-x}Al_xAg_{10}$ and (*b*) $Mg_{80-x}Al_xAg_{20}$ alloys. Open squares and circles represent the data for amorphous and quasicrystalline phases, respectively. Small solid circles represent the free electron value. (*c*) Temperature dependence of the Hall coefficient for the amorphous and quasicrystalline alloys. The numbers 1 and 2 denote the identification of the samples shown in figure 3(*a*).

3.2. Mg–Al–Cu

A first report on the formation of a quasicrystal in the Mg–Al–Cu alloy system was made by Sastry *et al* (1986), followed by further detailed studies on both structural (Shen *et al* 1988, Sakurai *et al* 1988) and physical properties (Bruhwiler *et al* 1988). The composition range, where the quasicrystalline single phase has been obtained, is summarised in figure 5, including the data in the literature (Cassada *et al* 1986, Shibuya *et al* 1988). The quasicrystalline single phase alloys obtained in the present experiment are expressed in the form of $Mg_{39.5}Al_{60.5-x}Cu_x$ (x = 6.5, 9.4, 12.3 and 15.2) and $Mg_xAl_{87.7-x}Cu_{12.3}$ (x = 35.8 and 43.2).

The low-temperature specific heat data in this alloy system can also be fitted to equation (1). The ratio $\gamma_{exp}/\gamma_{free}$ is found to be close to 1.2, indicating again the validity of the free electron approximation. Here Cu, Mg and Al are assumed to donate 1, 2 and 3 valence electrons per atom, respectively. The composition dependence of γ is small, as will be discussed in the section 4.4.

The ρ–T curves for the typical Mg–Al–Cu quasicrystals measured in the range 2–300 K are displayed in figure 6, along with the resistivity value at 300 K, which is shown in the inset. The resistivity is found to decrease with increasing Al content.

The temperature dependence of the Hall coefficient and the thermoelectric power is studied for all Mg–Al–Cu quasicrystals. It is found that the Hall coefficient exhibits a

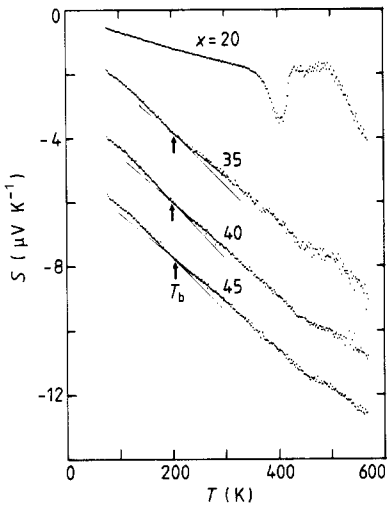

Figure 4. Temperature dependence of the thermoelectric power for the $Mg_{90-x}Al_xAg_{10}$ alloys. The sample with $x = 20$ is amorphous, whereas those with $x = 35$, 40 and 45 are quasicrystalline. The data for $x = 40$ and 45 are displaced downwards by 2 and 4 μV K^{-1}, respectively, to avoid superposition of the data points. Two straight lines are drawn to approximate the non-linear temperature dependence below 300 K. An arrow indicates the intersection of two lines and is referred to as a characteristic temperature T_b. Complex temperature dependences above 300 K are most likely influenced by the structural relaxation and the crystallisation effects

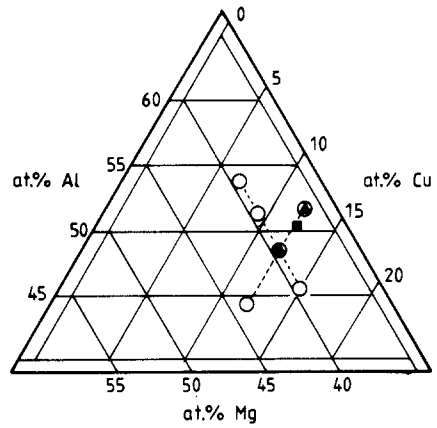

Figure 5. Composition range for the formation of the icosahedral quasicrystalline single phase in the Mg–Al–Cu alloy system. (○): present results; (■): Cassada *et al* (1986), (▲): Shibuya *et al* (1988). Dashed lines refer to the alloy formula $Mg_{39.5}Al_{60.5-x}Cu_x$ and $Mg_xAl_{87.7-x}Cu_{12.3}$.

measurable temperature dependence, whenever the Hall coefficient at 300 K deviates from the free electron value. The data for the thermoelectric power below 300 K can again be fitted to two straight lines in the same manner as those shown in figure 4 for the Mg–Al–Ag quasicrystals.

3.3. Mg–Zn–Ga

The composition range for the formation of an icosahedral quasicrystalline phase in the Mg–Zn–Ga system is shown in figure 7. The literature data are also included (Chen and Inoue 1987, Shibuya *et al* 1988, Ohashi and Spaepen 1987). Ohashi and Spaepen pointed out that an icosahedral phase of the $Ga_{1.0}Mg_{1.8}Zn_{2.1}$ alloy prepared by melt spinning is stable up to the melting temperature. In the present experiments, the quasicrystalline alloy $Mg_{39.5}Zn_{40}Ga_{20.5}$ or $Ga_{1.0}Mg_{1.92}Zn_{1.95}$ in their expression turned out to be stable up to the temperature quite close to the melting point. This was identified from the lack of any transformation in both DSC and resistivity measurements. More surprisingly, as shown in figure 8, the x-ray diffraction lines characteristic of a quasicrystalline phase become much sharper due to the heat treatment. The same measurements were made on the quasicrystalline sample with the composition employed by Ohashi and Spaepen. However, it crystallised before melting. The best quasicrystallinity in the present

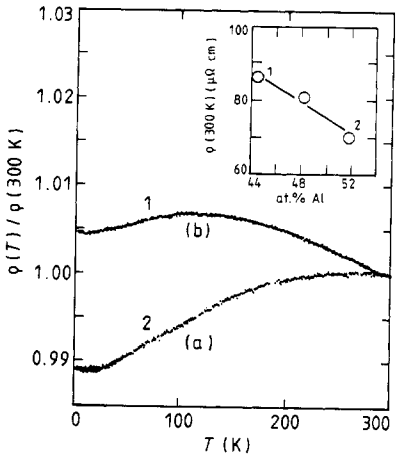

Figure 6. Temperature dependence of the electrical resistivity normalised with respect to that at 300 K for the quasicrystalline Mg–Al–Cu alloys. Inset shows the Al concentration dependence of the resistivity at 300 K for the quasicrystalline $Mg_xAl_{87.7-x}Cu_{12.3}$ alloys. The number denotes the identification of the samples shown in the inset. The letters (a) and (b) denote the ρ–T types discussed in section 4.1.

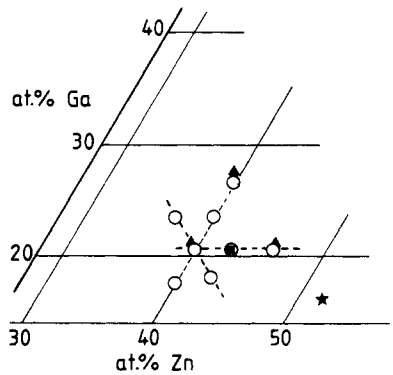

Figure 7. Composition range for the formation of the quasicrystalline single phase in the Mg–Zn–Ga alloy system. (○): present results, (▲): Shibuya *et al* (1988); (★): Chen and Inoue (1987) and (■): Ohashi and Spaepen (1987). The three dashed lines refer to the alloys $Mg_{60-x}Zn_{40}Ga_x$, $Mg_{39.5}Zn_{60.5-x}Ga_x$ and $Mg_{79.5-x}Zn_xGa_{20.5}$.

measurements was achieved at the composition slightly different from that reported by Ohashi and Spaepen. A sharpness of the diffraction lines is most likely brought about by the growth of the quasicrystalline grains and the reduction in the phasons and other defects present in the as-quenched sample.

The low-temperature specific heat data can be fitted to equation (1). The value of γ_{free} is calculated by assuming that Mg, Zn and Ga release 2, 2 and 3 valence electrons per atom as the free electrons, respectively. The ratio $\gamma_{exp}/\gamma_{free}$ in this system is found to be distributed over 0.75 to 1.14, being definitely smaller than the value of 1.2 observed in the other two alloy systems already mentioned. A smaller ratio suggests that the deviation from the free electron model is not negligible in the present system. Very recently, Wagner *et al* (1989) reported the value of γ_{exp} of 0.18 mJ mol^{-1} K^{-2} for the icosahedral $Mg_{32}Zn_{52}Ga_{16}$ alloy. Their value is extremely small, compared with the values of 0.80–0.99 mJ mol^{-1} K^{-2} found in the present measurements. The difference will be discussed in section 4.1.

The ρ–T curve together with the value of ρ against Ga content is shown in figure 9. The resistivity at 300 K is always higher than 140 $\mu\Omega$ cm and tends to increase with increasing trivalent Ga. Unfortunately, the $Mg_{33.5}Zn_{46}Ga_{20.5}$ quasicrystal possessing the largest resistivity in this family, 183 $\mu\Omega$ cm, broke during cooling, in spite of several attempts, and, hence, the data obtained were limited only down to 130 K. Regarding the Hall coefficient, the general rule mentioned above holds true again: it exhibits a measurable temperature dependence only for samples in which the value of R_H deviates from the corresponding free electron value. The temperature dependence of the thermoelectric power has also been studied and the non-linear temperature dependence is again observed below 300 K in this series of alloys (Matsuda *et al* 1990).

4. Discussion

4.1. Electrical resistivity in quasicrystals

The temperature dependence of the electrical resistivity for the sp-electron quasicrystals shown in figures 2, 6 and 9 is firstly discussed. As will be shown below, the ρ–T curves

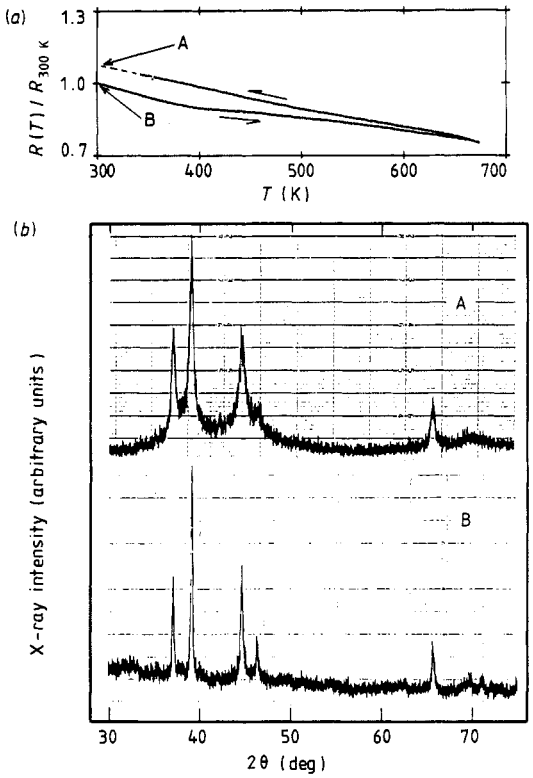

Figure 8. Temperature dependence of the electrical resistivity normalised with respect to that at 300 K for the quasicrystalline $Mg_{39.5}Zn_{40}Ga_{20.5}$ alloy. An arrow indicates the direction of heating and cooling with the heating rate of 10 K min^{-1}. The x-ray diffraction profiles are shown at the bottom for (*a*) the as-quenched sample A, (*b*) the sample B heated up to 673 K just below the melting point.

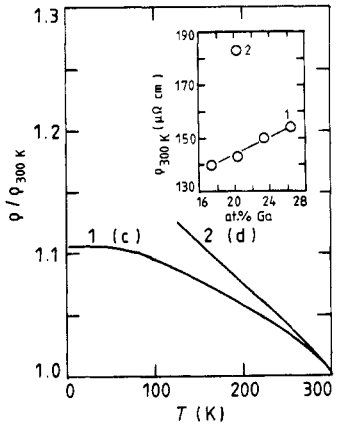

Figure 9. Temperature dependence of the electrical resistivity normalised with respect to that at 300 K for the quasicrystalline Mg–Zn–Ga alloys. The number denotes the identification of the samples shown in the inset. Inset shows the Ga concentration dependence of the resistivity at 300 K for the quasicrystalline $Mg_{60-x}Zn_{40}Ga_x$ and $Mg_{33.5}Zn_{46}Ga_{20.5}$ (No 2 in the inset) alloys. The letters (c) and (d) denote the ρ-T types discussed in section 4.1.

observed for the present quasicrystals possess essentially the same features as those found for the non-magnetic amorphous alloys. It is, therefore, worthwhile describing the ρ–T characteristics in the amorphous alloys.

It has been pointed out that any ρ–T curve below approximately 300 K for non-magnetic amorphous alloys can be described by one of the five representative types (a) to (e) and changes in this alphabetical order with increasing resistivity in a given alloy system (Mizutani 1988a, b). Type (a) possesses a feature such that the resistivity increases quadratically at low temperatures and almost linearly above about 200 K. Type (b) is viewed as type (a) being progressively taken over by the region with a negative TCR at high temperatures. Thus, the type (b) is characterised by a resistivity maximum at an intermediate temperature range. A negative TCR eventually dominates over an entire

temperature range: a decreasing quadratic temperature dependence at low temperatures and a more or less linear one at higher temperatures. This is designated as type (c). It has been shown that the types (a), (b) and (c) and a change in this sequence with increasing resistivity can be well interpreted in terms of the generalised Faber–Ziman theory based on the ordinary Boltzmann transport equation with the dynamical structure factor incorporated.

Further increase in resistivity results in further change in the ρ–T characteristics. The quadratic temperature dependence is lost at low temperatures and the ρ–T curve approaches more or less a straight line over a wide temperature range. We call this type (d). When the resistivity further increases, the curvature changes and the ρ–T curve becomes concave downwards. This is called type (e). Type (e) is observed in the sp-electron amorphous alloys with resistivity exceeding about 500 $\mu\Omega$ cm and also in the d-electron amorphous alloys. It was emphasised that both types (d) and (e) appear only when the mean free path of the conduction electrons becomes comparable with the average atomic distance and the scattering mechanism based on the ordinary Boltzmann transport equation breaks down. The role of the weak localisation is claimed to be important in this high-resistivity regime (Mizutani 1988a, b).

As shown in figures 2, 6 and 9, all ρ–T data for quasicrystals can be grouped in terms of the types observed in the non-magnetic amorphous alloys. The mean free path of conduction electrons generally becomes comparable with the average atomic distance of about 4–5 Å at the resistivity of about 200 $\mu\Omega$ cm (Mizutani 1988a, b). It happened that all sp-electron quasicrystals studied in this experiment possess relatively low resistivities below 200 $\mu\Omega$ cm. Indeed, all ρ–T data can be described in terms of types (a), (b) and (c) except in the case of $Mg_{33.5}Zn_{46}Ga_{20.5}$ with resistivity 183 $\mu\Omega$ cm, which may be better assigned to type (d) (Matsuda *et al* 1990). It is also worth emphasising that the types appear in alphabetical sequence with increasing resisitivity. Kimura *et al* (1989) observed type (d) for the $Al_{55.0}Li_{35.8}Cu_{9.2}$ quasicrystal with resistivity exceeding 800 $\mu\Omega$ cm. Using the measured electronic specific heat coefficient of $\gamma_{exp}/\gamma_F = 0.39$ as a guide, they suggested that a substantial reduction in the carrier density at the Fermi level coupled with the shortest mean free path limited by the average atomic distance is most likely responsible for the occurrence of the ρ–T curve of type (d).

It is surprising that types (a) to (d) appear in this order with increasing resistivity for sp-electron quasicrystals in exactly the same manner as found in the sp-electron amorphous alloys. Indeed, it is not *a priori* obvious that the generalised Faber–Ziman theory is applicable to the sp-electron quasicrystals even in the low-resistivity regime. We pointed out in figure 8 that the resistivity for the $Mg_{39.5}Zn_{40}Ga_{20.5}$ quasicrystal *increased* by about 8% upon heating almost up to the melting point and that its increase was accompanied by a substantial sharpening of the x-ray diffraction peaks. This apparently contradicts the prediction from the generalised Faber–Ziman theory, since a sharpening of the structure factor would naturally contribute to reduce the resistivity. Sokoloff (1987) pointed out on the basis of the perturbation theory that if quasicrystals could be made which had fewer defects or which did not have d states near the Fermi level, their resistivity should be fairly small. The present Mg–Zn–Ga quasicrystal is entirely free from the d-electron conduction. We consider that the present findings hold a critical key role in the understanding of the scattering mechanism of the conduction electrons in the quasiperiodic lattice.

From the conductivity formula $\sigma = \rho^{-1} = (e^2/3)\Lambda_F v_F N(E_F)$, we naturally expect an inversely proportional relation between the measured resistivity ρ and the density of states at the Fermi level $N(E_F)$ or the electronic specific heat coefficient γ, provided that

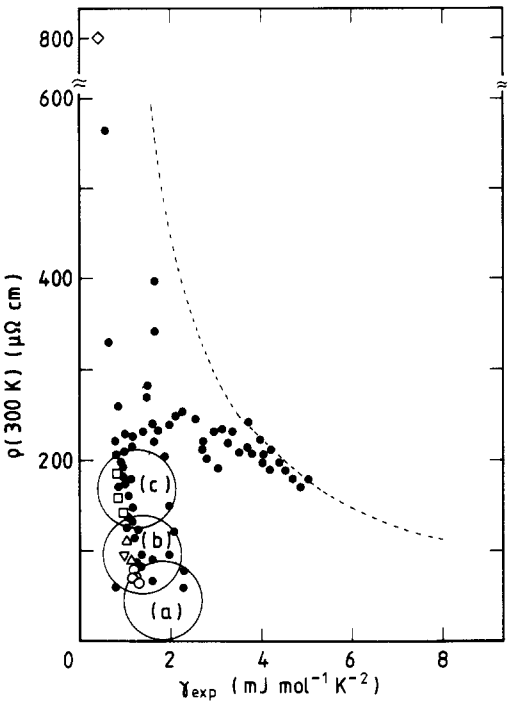

Figure 10. The interdependence of the electrical resistivity ρ(300 K) and the measured electronic specific heat coefficient γ_{exp} for non-magnetic amorphous and quasicrystalline alloys; (△): Mg–Al–Ag; (○): Mg–Al–Cu; (□): Mg–Zn–Ga; (▽): Mg–Al–Zn (Matsuda *et al* 1989) and (◇): Al–Li–Cu (Kimura *et al* 1989). The data for the amorphous alloys are reproduced from Mizutani *et al* (1990a) and shown by small solid circles. The data possessing the ρ-T types (a), (b) and (c) are encircled. The data outside the circles belong to either types (d) or (e). A dashed curve represents a possible high-resistivity limiting curve.

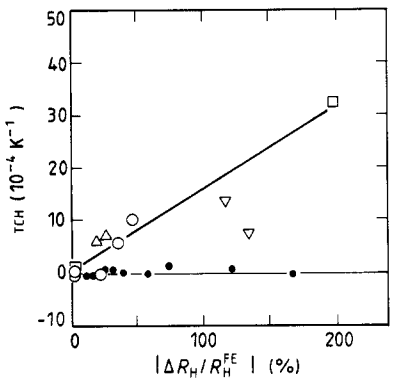

Figure 11. TCH as a function of the deviation of the measured Hall coefficient from the corresponding free electron value for the sp-electron quasicrystals; (△): Mg–Al–Ag; (○): Mg–Al–Cu; (□): Mg–Zn–Ga and (▽): Mg–Al–Zn (Matsuda *et al* 1989). The data for the sp-electron amorphous alloys are marked by smaller solid circles (Matsuda *et al* 1984, Mizutani and Matsuda 1984). The free electron value is calculated using the expression $R_H = -A/|e|N_A(e/a)d$, where e is the electronic charge, N_A is the Avogadro number, d is the measured density and e/a is the average valence electrons per atom.

the mean free path Λ_F and the Fermi velocity v_F become constant in a given alloy system. In the high-resistivity limit characterised by the types (d) or (e), the mean free path Λ_F would be limited by an average atomic distance of about 4–5 Å. The average Fermi velocity v_F is less certain but is estimated to be about one-fifth the free electron value in the d-electron system (Mizutani 1988a, b). The value of v_F in the sp-electron system may be more reliably estimated from the measured values of γ and the Hall coefficient.

Figure 10 reproduces the ρ–γ plots for non-magnetic amorphous alloys so far studied (Mizutani *et al* 1990a), onto which the data for the quasicrystals are superimposed. A hyperbolic dashed curve drawn represents the ρ–γ relation, where v_F is set to one-fifth of the free electron value of 10^8 cm s^{-1} and Λ_F is 4 Å in the conductivity formula above. Types (d) and (e) appear only in the neighbourhood of this limiting curve, whereas types (a), (b) and (c), the respective data of which are encircled, fall well below this curve. The data for the quasicrystals are still scarce. But, it is clear from figure 10 that the sp-electron quasicrystals fall on a steeply declining curve almost identical to that formed

by sp-electron amorphous alloys. This indicates that the electronic structure at E_F or the effective carrier concentration is largely responsible for the magnitude of the resistivity in both sp-electron amorphous and quasicrystalline alloys in spite of the significant difference in the above mentioned structure factor. Finally, a brief comment is made on the data recently reported by Wagner *et al* (1989). They obtained a small γ_{exp} value of 0.18 mJ mol^{-1} K^{-2} and a relatively low resistivity of 98 $\mu\Omega$ cm for the $Mg_{32}Zn_{52}Ga_{16}$ quasicrystal. Their data fall in an extremely unfavourable region in the ρ–γ plot in figure 10. Further accumulation of ρ–γ data is in progress to establish this interesting relationship in quasicrystals: a low resistivity less than about 100 $\mu\Omega$ cm always accompanies a free electron-like value of γ and the resistivity increases sharply with decreasing the value of γ relative to the free electron value.

4.2. Hall coefficient in quasicrystals

Figure 11 summarises the interrelation between the temperature coefficient of the Hall coefficient (TCH) defined as $(|1/R_H|)(dR_H/dT)$ near 300 K and the deviation of the Hall coefficient from the free electron value for sp-electron quasicrystals studied in this experiment, along with the data for the sp-electron amorphous alloys. Although the value of TCH is negligibly small in the amorphous alloys, it tends to increase almost linearly in the quasicrystals with increasing the deviation from the free electron value. This difference is surprising, since the ρ–T characteristics discussed above are seemingly quite similar to each other. The Fermi surface in the quasicrystals may well be distorted due to the presence of the Brillouin zone, as inferred from the strong Bragg reflections in the x-ray or electron diffraction spectra. The anisotropic Fermi surface and the resulting temperature-dependent anisotropy in the relaxation time of the conduction electrons is most likely responsible for the temperature dependence of the Hall coefficient.

4.3. Thermoelectric power in quasicrystals

It has been pointed out that the thermoelectric power of sp-electron quasicrystals studied in this experiment exhibits unique non-linear temperature dependence below 300 K. Its behaviour above 300 K is complex due, presumably, to the superposition of the structural relaxation and the crystallisation effects. All the data below 300 K were fitted to two straight lines below and above T_b (see figure 4). As shown in figure 12(*a*), the temperature T_b tends to increase with increasing resistivity. However, no correlation with the Debye temperature is apparently found, as indicated in figure 12(*b*), suggesting that the electron–phonon interaction would not be responsible for this unique temperature dependence. Further work is needed to clarify the mechanism of the non-linear temperature dependence of the thermoelectric power in the sp-electron quasicrystals.

4.4. Density of states at E_F in quasicrystals

The measured electronic specific heat coefficient γ_{exp} in sp-electron quasicrystals is plotted in figure 13 as a function of the nominal electron concentration $(e/a)_n$. Included are the data for the corresponding free electron value γ_{free}, which is calculated by using the measured density and the nominal electron concentration. First of all, it is seen that the sp-quasicrystals so far obtained fall in the limited e/a range of 2.1–2.5. Realising that the electron–phonon interaction enhances the value of γ by 20–30% in non-superconducting simple metals, we may reasonably quote the free electron regime as the

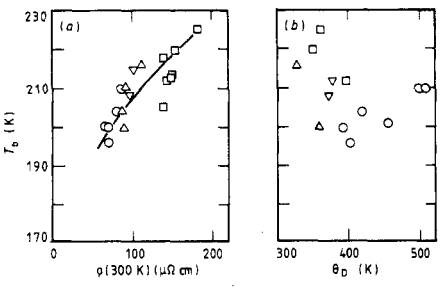

Figure 12. The characteristic temperature T_b deduced from the thermoelectric power data (see figure 4) as a function of (*a*) the resistivity at 300 K and (*b*) the Debye temperature for the various quasicrystals; (△): Mg–Al–Ag; (○): Mg–Al–Cu; (□): Mg–Zn–Ga and (▽): Mg–Zn–Al (Matsuda *et al* 1989).

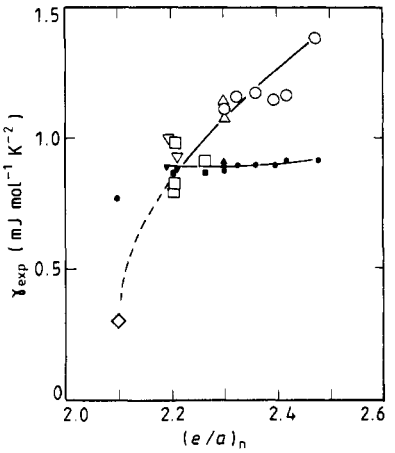

Figure 13. The measured electronic specific heat coefficient γ_{exp} as a function of nominal valence electrons per atom for various quasicrystals; (△): Mg–Al–Ag; (○): Mg–Al–Cu; (□): Mg–Zn–Ga; (▽): Mg–Zn–Al (Matsuda *et al* 1989) and (◇): Al–Li–Cu (Kimura *et al* 1989). The corresponding free electron value marked by smaller solid symbols is calculated using equation (2) in the text.

composition range where the ratio $\gamma_{exp}/\gamma_{free}$ is around 1.2–1.3. In other words, the ratio close to or smaller than unity indicates the region where the density of states at E_F is lowered below the free electron value.

Figure 13 indicates that the value of γ_{exp} falls on a single curve with a positive slope, regardless of the alloy systems, and that its slope is much steeper than that of the free electron curve. As a result, the deviation from the free electron behaviour becomes more significant, as $(e/a)_n$ is lowered below 2.2. Indeed, the value of γ_{exp} for the Al–Li–Cu quasicrystal reaches only 0.3 mJ mol^{-1} K^{-2} (Kimura *et al* 1989, Wagner *et al* 1989).

Fujiwara (1989) recently calculated the electronic density of states for a cubic $Al_{114}Mn_{24}$ crystalline alloy analogous to the quasicrystal by the linear muffin-tin orbital-atomic-sphere approximation coupled with the local-density-functional method. It turns out that the Mn 3d states form the sharp resonance and antiresonance peaks and that the Fermi level happens to fall in the resulting pseudogap or the density of states minimum. He suggested that the location of the Fermi level in the density of states minimum contributes to stabilise the icosahedral structure. A small γ_{exp} value for the Al–Li–Cu quasicrystal implies that a deep valley exists in the density of states curve and the Fermi level sits near its minimum. Although the origin of the minimum is definitely different from that in Al–Mn discussed above, the coincidence of the Fermi level with the minimum would assist to stabilise the icosahedral structure. Indeed, the Al–Li–Cu quasicrystal is known to grow as a stable phase by casting the molten alloy in an iron mould with a subsequent annealing at 800 °C (Kimura *et al* 1989). Wagner *et al* (1989) also claimed the possession of small γ_{exp} values in the thermally stable Al–Cu–Fe, Mg–Zn–Ga and Al–Li–Cu quasicrystals and discussed the phase stability in terms of the Fermi surface–Brillouin zone interaction in the icosahedral structure.

The $Mg_{39.5}Zn_{40}Ga_{20.5}$ quasicrystal in the present experiment turned out to be stable up to the melting point and its quasicrystallinity improved after the heat treatment.

However, the value of γ_{exp} for this particular sample is not necessarily the smallest among thermally less stable quasicrystals in this alloy system. Further work is of particular interest to ascertain more conclusively if a reduced density of states at the Fermi level is a characteristic feature of a thermally stable quasicrystalline alloy. The electron transport properties, including the low-temperature specific heats, have been measured for the thermodynamically stable Al–Cu–Ru icosahedral quasicrystals, whose preparation had been first reported by Tsai *et al* (1989). The results are presented in the following paper (Mizutani *et al* 1990b).

5. Conclusion

The electronic structure and electron transport properties have been studied for a large number of sp-electron quasicrystals in the three alloy systems Mg–Al–Ag, Mg–Al–Cu and Mg–Zn–Ga. It turns out that the characteristic feature of the ρ–T type, its systematic change with increasing resistivity and the ρ–γ plot behave in the same manner as those established earlier for the non-magnetic amorphous alloys. This is consistent with the prediction from the generalised Faber–Ziman theory. However, a definite increase in resistivity upon improvement in the quasicrystallinity due to the heat-treatment casts a doubt on this simple interpretation, provided that only the sharpening in the structure factor is taken into consideration. The temperature dependence of the Hall coefficient and the thermoelectric power is unique in the quasicrystalline phase. The former is discussed in terms of the Fermi surface–Brillouin zone interaction. The electronic specific heat coefficient is found to exhibit a universal trend over the e/a range of 2.1–2.5 and to decrease rapidly with decreasing e/a. A thermally stable quasicrystal tends to possess a reduced density of states at the Fermi level, suggesting its important role in stabilising the quasiperiodic icosahedral structure.

Acknowledgments

The authors are grateful to Professor J Hafner, Technical University of Vienna, for fruitful discussions on the applicability of the generalised Faber–Ziman theory for the low-resistivity sp-electron quasicrystals. They also wish to express their thanks to Messrs. S Ohashi, I Ohara, K Nakamura, M Nakamura and A Kamiya for their experimental assistance.

References

Bruhwiler P A, Wagner J L, Biggs B D, Shen Y, Wong K M, Schnatterly S E and Poon S J 1988 *Phys. Rev.* B **37** 6529

Cassada W A, Shen Y, Poon S J and Shiflet G J 1986 *Phys. Rev.* B **34** 7413

Chen H S and Inoue A 1987 *Scr. Metall.* **21** 527

Fujiwara T 1989 *Phys. Rev.* B **40** 942

Inoue A, Nakano K, Bizen Y, Masumoto T and Chen H S 1988 *Japan. J. Appl. Phys.* **27** L944

Kimura K, Iwahashi H, Hashimoto T, Takeuchi S, Mizutani U, Ohashi S and Itoh G 1989 *J. Phys. Soc. Japan* **58** 2472

Matsuda T, Ohara I, Sato H, Ohashi S and Mizutani U 1989 *J. Phys.: Condens. Matter* **1** 4087

Matsuda T, Sakabe Y, Ohara I and Mizutani U 1990 *Proc. 7th Int. Conf. on Liquid and Amorphous Metals (Kyoto, 1989); J. Non-Cryst. Solids* **117 + 118** 804

Matsuda T, Shiotani N and Mizutani U 1984 *J. Phys. F: Met. Phys.* **14** 1193
Mizutani U 1988a *Mater. Sci. Eng.* **99** 165
—— 1988b *Trans. Japan. Inst. Met. Suppl.* **29** 275
Mizutani U and Matsuda T 1984 *J. Phys. F: Met. Phys.* **14** 2995
Mizutani U, Ohashi S, Matsuda T, Fukamichi K and Tanaka K 1990a *J. Phys.: Condens. Matter* **2** 541
Mizutani U, Sakabe Y, Shibuya T, Kishi K, Kimura K and Takeuchi S 1990b *J. Phys.: Condens. Matter* **2** 6169
Ohashi W and Spaepen F 1987 *Nature* **330** 555
Sakurai Y, Kokubu C, Tanaka Y, Watanabe Y, Masuda M and Nanao S 1988 *Mater. Sci. Eng.* **99** 423
Sastry G V S, Rao V V, Ramachandrarao P and Anantharaman T R 1986 *Scr. Metall.* **20** 191
Shen Y, Dmowski W, Egami T, Poon S J and Shiflet G J 1988 *Phys. Rev.* B **37** 1146
Shibuya T, Kimura K and Takeuchi S 1988 *Japan. J. Appl. Phys.* **27** 1577
Sokoloff J B 1987 *Phys. Rev.* B **36** 6361
Steinhardt P J and Ostlund S 1987 *The Physics of Quasicrystals* (Singapore: World Scientific) pp 1–136
Tsai A P, Inoue A and Masumoto T 1989 *Japan. J. Appl. Phys.* **27** L1587
Wagner J L, Biggs B D, Wong K M and Poon S J 1988 *Phys. Rev.* B **38** 7436
Wagner J L, Wong K M and Poon S J 1989 *Phys. Rev.* B **39** 8091